Article

J. Biol. Regul. Homeost. Agents. 2025; 39(1): 79–88
https://doi.org/10.23812/j.biol.regul.homeost.agents.20253901.10

Effects of Histone Deacetylase 2 on Epithelial-Mesenchymal Transition in Pulmonary Fibrosis

Yu Liu[1,2], Songjun Shao[3], Yu Tan[4], Shanyu Wang[4], Peng Zheng[4], Jing Han[3], Ying Zhao[3], Shanshan Rao[1,3,*]

[1]Department of Biology and Medicine, Medical School, Guizhou University, 550025 Guiyang, Guizhou, China
[2]Nrational Health Commission Key Laboratory of Pulmonary Immunological Diseases, Guizhou Provincial People's Hospital, 550002 Guiyang, Guizhou, China
[3]Department of Respiratory and Critical Care Medicine, Guizhou Provincial People's Hospital, 550002 Guiyang, Guizhou, China
[4]Department of Respiratory Medicine, The First Clinical College of Zunyi Medical University, 563006 Zunyi, Guizhou, China
*Correspondence: raoshan3@126.com (Shanshan Rao)
Submitted: 15 November 2024 Revised: 2 December 2024 Accepted: 17 December 2024 Published: 16 January 2025

Background: Pulmonary fibrosis (PF) is a chronic and progressive interstitial lung disease. Histone deacetylases (HDACs) play a crucial role in the onset and development of PF. Changes in HDACs 1–10 expression levels occur during PF development, and their specific roles remain unclear. Therefore, we elucidated changes in the gene and protein levels of HDACs 1–10. Furthermore, we selectively knocked down HDAC2 to explore the molecular mechanism underlying the regulatory role of HDAC2 in epithelial-mesenchymal transition (EMT) during the development of PF.

Methods: Lewis lung carcinoma (LLC) cells were stimulated with transforming growth factor-β1 (TGF-β1) (5 ng/mL) to establish a lung fibrosis cell model. Additionally, C57BL/6 mice received bleomycin through single intratracheal instillation at a 3.5 mg/kg volume, diluted in 0.7 mL saline. Furthermore, EMT-related gene and protein expression levels were assessed using quantitative PCR (qPCR) and Western blotting, respectively.

Results: We observed that HDAC2 expression levels were significantly increased in both the *in vitro* and *in vivo* PF models. HDAC2 knockdown significantly decreased the expression levels of fibrosis indicators such as collagen type I (Col-I) and collagen type IV (Col-IV), and EMT indicator α-smooth muscle actin (α-SMA) was observed. Conversely, it increased the expression of EMT indicator E-cadherin (E-cad). Hematoxylin and eosin (H&E) and Masso staining revealed that HDAC2 knockdown substantially reduced the degree of pulmonary fibrosis. These findings suggest that lowering HDAC2 expression inhibits EMT and reduces PF. Moreover, in a TGF-β1-induced lung fibrosis cell model, HDAC2 knockdown significantly reduced epithelial growth factor receptor levels, which inhibited mitogen-activated protein kinases (MAPK) signaling and decreased the protein expression of p38 and c-Jun N-terminal kinase (JNK).

Conclusions: HDAC2 knockdown effectively impedes EMT and diminishes PF severity, impacting the JNK/p38 MAPK signaling pathway, which may serve an inhibitory function.

Keywords: pulmonary fibrosis; HDAC2; epithelial-mesenchymal transition; JNK/p38 MAPK signaling pathways

Background

Pulmonary fibrosis (PF) is a progressive interstitial disease of the lung tissue. PF involves epithelial-mesenchymal transition (EMT) and the proliferation and activation of myofibroblasts [1]. This disease has an unclear etiology and extremely poor prognosis, with a median survival of less than three years after diagnosis [2]. Treating PF is challenging, and the World Health Organization classifies it as a difficult-to-treat lung disease [3].

Histone deacetylases (HDACs), important gene regulatory factors in many biological processes [4], constitute a class of proteases. In normal physiological conditions, histone acetylation and deacetylation processes within the nucleus are balanced through histone acetyltransferase (HAT) and HDACs [5]. HDACs have been associated with the onset and progression of PF [6]. The development of fibrosis in many organs, including heart, kidney, lung, and liver, has been closely linked to EMT [7]. Transforming growth factor-β1 (TGF-β1) is crucial in inducing EMT fibrosis site [8]. Class I and II HDACs may promote fibrosis progression, whereas class III may exert a negative regulatory effect. For example, significantly elevated HDAC1-5 and HDAC8 protein expressions have been reported in renal tubular epithelial cells of TGF-β1-treated rat and a rat model of renal fibrosis, with HDAC2 ex-

Journal of
BIOLOGICAL REGULATORS
and Homeostatic Agents

hibiting particularly substantial upregulation [9]. In TGF-β1-treated human skin fibroblasts, silencing of HDAC1-8 using a small interfering RNA (siRNA) technique revealed impaired TGF-β1-induced α-smooth muscle actin (α-SMA) expression when HDAC4, HDAC6, and HDAC8 were silenced [10]. Furthermore, HDAC4 silencing in the skin fibrosis cell model has been shown to significantly reduce α-SMA expression and inhibit TGF-β1-mediated EMT, suggesting the strongest fibrogenic effect of HDAC4 among HDAC1-8. Sirtuin (SIRT) 6, a member of class III HDACs, has been reported to inhibit bleomycin-induced EMT in mouse lungs [11]. Additionally, histone deacetylase inhibitors (HDACi) have been reported to have potential antifibrotic effects in the liver, skin, and heart. Several factors, including TGF-β1, activate p38/c-Jun N-terminal kinase (JNK), and the p38/JNK mitogen-activated protein kinases (MAPK) signaling pathway, play an important role in stress responses such as inflammation and apoptosis [12].

Class I and II HDACs play significant roles in organ fibrosis. For example, overexpression of HDAC3 has been found to promote renal fibrosis [13], and upregulation of HDAC6 expression has been observed in cardiac fibrosis [14]. However, the changes in HDACs 1–10 expression levels and their role in the development of PF have not been investigated [15]. Additionally, the predominant HDAC involved in the development of PF and its underlying mechanisms remain undetermined [16]. Therefore, this study aimed to explore changes in the expression levels of HDACs 1–10 during the development of fibrosis using lung fibrosis cell and lung fibrosis animal models. Furthermore, we assessed changes in fibrosis and EMT markers following relevant HDAC knockdown. Finally, we also investigated the involvement of the JNK/p38 MAPK signaling pathway in PF.

Materials and Methods

Treatment of LLC Cells

Lewis lung carcinoma (LLC) cell line is widely used in investigating lung diseases and EMT progression [17]. We obtained an LLC cell line from Pricella (CL0140, Wuhan, China). The cell line was cultured in PMI-50210 culture medium supplemented with 1% penicillin-streptomycin (PM150210, Pricella, Wuhan, China) and 10% fetal bovine serum (164210-50, Pricella, Wuhan, China) and incubated in a humidified environment at 37 °C and 5% CO_2. The cell cultures were examined for contamination using mycoplasma testing and authenticated utilizing short tandem repeat (STR) analysis. Moreover, EMT was induced in these cells utilizing TGF-β1 (5 ng/mL). Cell treatment with TGF-β1 followed a previously described protocol [18].

In Vitro Experiment

The cells were randomly divided into various groups as follows: LLC and LLC+TGF-β1 groups, and LLC, virus, HDAC2 virus, TGF-β1+virus, and TGF-β1+HDAC2 virus groups. Each set of experiments was repeated three times. Cells were exposed to 5 ng/mL of TGF-β1 based on their respective groups. After 24 hours of incubation, total protein was extracted from the cells and underwent quantification. Moreover, the initial cell density was 5×10^5, and the final collected cell density was 1×10^6.

In Vivo Experiments

Thirty C57BL/6 mice (half males and half females), aged 6–8 weeks and weighing 19–22 g, were randomly divided into Normal group (NC), virus, HDAC2 virus, bleomycin (BLM)+virus, and BLM+HDAC2 virus groups, each comprising 6 mice. They were housed in a controlled environment at 25 °C with a 12-hour dark/light cycle. Furthermore, they were provided standard chow for 7 days before the experiments and had free access to water.

Twelve mice were randomly divided into NC and NC+BLM groups, with equal representation of males and females in each group. The NC received 0.7 mL of saline through trachea instillation. However, the BLM group of mice received bleomycin at a dose of 3.5 mg/kg per mouse, diluted in 0.7 mL saline, and delivered through the trachea instillation. After 28 days of modeling, mice were anesthetized to death with 3% sodium pentobarbital (150 mg/kg). lung tissues were surgically excised for PCR and WB analyses to determine changes in gene transcript and protein levels of class I and II HDACs (HDAC1–10) expression in lung tissues of both groups. This analysis aimed to validate whether the findings were consistent with those observed in the *in vitro* experiments.

After this, C57 mice (n = 30) were randomly divided into the following groups (each comprising 6 mice): the NC group (administered with a single tracheal instillation of 0.7 mL saline), the Virus group (received an injection of 50 µL of control interfering virus), the HDAC2 virus group (received an injection of 50 µL of HDAC2 control interfering virus), the BLM+virus group (administered with 3.5 mg/kg bleomycin diluted in 0.7 mL saline and delivered through single intratracheal instillation followed by an injection of 50 µL control interfering virus), and the BLM+HDAC2 virus group (administered with 3.5 mg/kg bleomycin diluted in 0.7 mL of saline and delivered through single intratracheal instillation followed by an injection of 50 µL HDAC2 control interfering virus). After 28 days of modeling, mice were anesthetized to death with 3% sodium pentobarbital (150 mg/kg). These lung tissues underwent various analyses, including H&E staining, Masson staining, hydroxyproline content of mouse lung tissues, immunofluorescence staining, Western blot analysis, to determine the levels of α-SMA, E-cadherin (E-cad), CoI-I, and CoI-IV, and quantitative PCR (qPCR) to assess the mRNA expression of α-SMA, E-cad, CoI-I, and CoI-IV. The success rate of our experiment was 86%.

All mice received proper care, following the animal laboratory guidelines [19]. The study design was approved by the Animal Ethics Committee of Guizhou Medical University, China (No. 2101491) on 8 August 2021.

Specimen Collection and Histopathological and Immunohistochemical Examination

Tissues were collected and underwent dehydration in a biological tissue dehydrator and subsequently washed. After this, they were embedded in paraffin and processed for histological examination. For this purpose, tissues were sectioned into 3 µm thick slices to assess pulmonary fibrosis using hematoxylin and eosin (H&E) and Masson's trichrome stain [20]. Finally, the stained tissue slices were examined utilizing a microscope (ECLIPSE Ts2, Nikon, Tokyo, Japan) to determine the extent of fibrosis.

Quantitative PCR

The expression levels of HDAC2 and fibrogenesis-related genes were evaluated using qPCR. β-actin was employed as an endogenous control. For this purpose, total RNA was extracted using TRIzol (15596026CN, Invitrogen, Shanghai, China). RNA concentration was assessed using a spectrophotometer [21] and subsequently converted into cDNA using a HiScript II reagent Kit (R223-01, VAZYME, Nanjing, China) with a gDNA eraser. Moreover, qPCR was performed using a SYBR Green qPCR kit (Q111-02, VAZYME, Nanjing, China) and gene-specific primers following the manufacturer's instructions. The expression levels of target genes were determined using the $2^{-\Delta\Delta Ct}$ method [22].

The primers used in qPCR were as follows: *β-actin* positive strand, CACGATGGAGGGGCCGGACTCATC; Mus *β-actin* negative strand, TAAAGACCTCTATGCCAACACAGT; Mus *HDAC2* positive strand, GATGGAGAAGACCCGGACAA; *HDAC2* negative strand, TGGGGTCTGTTTTCTCACCA. Mus *a-SMA* positive strand, CTTCGCTGGTGATGATGCTC, Mus *a-SMA* negative strand, GTTGGTGATGATGCCGTGTT; Mus *E-cad* positive strand, ACTTTGGTGTGGGTCAGGAA; Mus *E-Cad* negative strand, CACATGCTCAGCGTCTTCTC; Mus *Col-I* (collagen I) positive strand, CCTGGCAAAGACGGACTCAAC; Mus collagen type I (*Col-I*) negative strand, GCTGAAGTCATAACCGCCACTG; Mus collagen type IV (*Col-IV*) positive strand, AAGGACAAATCGGACCCACT; Mus *Col-IV* negative strand, AAGCCCATTCCTCCAACTGA.

Western Blotting

Following TGF-β1 stimulation and BLM induction, total protein was extracted from the cells and mice tissues. After centrifugation (12,000 rpm) at 4 °C for 10 minutes, protein content was quantified in the resultant supernatant utilizing a BCA kit (P0011, Beyotime, Shanghai, China) [23]. A 40 µg protein sample was resolved on Tris-Base 5% protein gels (17296, Invitrogen, Shanghai, China) and subsequently transferred onto polyvinylidene difluoride (PVDF) membranes. The membrane was blocked with 5% skimmed milk at room temperature for 1 hour and washed with TBST. After this, membrane was incubated overnight with primary antibodies, including anti-β-actin (1:500, BM0627, Boster, Wuhan, China), anti-α-SMA (1:1000, AF1032, Affinity, Liyang, China), anti-E-cad (1:1000, AF0131, Affinity, Liyang, China), anti-collagen-I (1:1000, AF7001, Affinity, Liyang, China), anti-collagen-IV (1:1000, AF0510, Affinity, Liyang, China), or anti-HDAC2 (1:1000, AF6470, Affinity, Liyang, China) at 4 °C. The next day, the membrane was incubated with HRP-labeled sheep anti-rabbit secondary antibody (1:10,000, AF0131, Affinity, Liyang, China) [24]. After washing, protein bands on the membranes were visualized utilizing chemiluminescent reagents and observed using a UVP imaging system (Gelodoc-it2310, Thermo Fisher Scientific Inc., Upland, CA, USA). Finally, protein bands were quantified and analyzed using Image J software (version 1.48 v; National Institutes of Health, Bethesda, MD, USA). Importantly, each immunoblot experiment was replicated three times.

Virus Target Screening

Three siRNA plasmids targeting *HDAC2* mRNA, including Hdac2-mus-231, Hdac2-mus-1021, and Hdac2-mus-1428, were designed and constructed. These expression vectors were transfected into LLC cells, and fluorescence was observed with a fluorescence microscope after 48 hours [25]. LLC cells were seeded into 6-well plates and incubated overnight. The cells were allowed to adhere to the culture plate walls and were infected with siRNA plasmids. The culture medium was changed 2 hours before infection, and the virus was added at a ratio of 1:50 of the multiplicity of infections (MOI). Reverse transcription qPCR was performed 48 hours after infection. Each experiment was repeated three times [26]. The primers used in qPCR were as follows: *HDAC2* positive strand, 5′-GATGGAGAAGACCCGGACAA-3′; *HDAC2* negative strand, 5′-TGGGGGTCTGTTTTCTCACCA-3′ Glyceraldehyde-3-phosphate dehydrogenase (*GAPDH*) positive strand, 5′-ATGGGTGTGAACCACGAGA-3′; and *GAPDH* negative strand, 5′-CAGGGGATGATGTTCTGGGGCA-3′.

Finally, the constructed adenoviral vector was transfected into cells at an MOI of 50. After this, 50 µL of the transfected cells were injected into each mouse for *HDAC2* knockdown.

Statistical Analyses

Statistical analyses were performed using GraphPad Prism 9.0 (GraphPad Software, San Diego, CA, USA). The differences between the two groups were compared using a *t*-test, and multiple group comparisons were conducted

Journal of
BIOLOGICAL REGULATORS
and Homeostatic Agents

using a one-way analysis of variance (ANOVA) [27]. Statistical significance was defined as $*p < 0.05$, $**p < 0.01$, $***p < 0.001$, and $****p < 0.0001$.

Results

TGF-β1 and BLM-Induced EMT Leading to Pulmonary Fibrosis

The induction of EMT and pulmonary fibrosis by TGF-β1 and BLM was verified through *in vivo* and *in vitro* experiments utilizing LLC cells and C57BL/6 mice, respectively. Markers of EMT and fibrosis were assessed in cells and lung tissues. After TGF-β1 treatment, the protein expression level of the epithelial cell marker E-cad was significantly reduced in LLC cells during the EMT transition of pulmonary fibrosis. In contrast, the protein expression level of the mesenchymal cell marker α-SMA was significantly increased (Fig. 1A, $p < 0.0001$). The protein expression levels of Col-I and Col-IV were increased in LLC cells after TGF-β1 stimulation (Fig. 1B,C, $p < 0.0001$ for Col-I and $p < 0.01$ for Col-IV). These findings suggest that TGF-β1 markedly promotes EMT in LLC cells. Additionally, BLM treatment facilitated changes in EMT and pulmonary fibrosis markers in mice (Fig. 1D–F).

Effects of Pulmonary Fibrosis on the Expression of HDAC1-10

The expression levels of HDACs were compared between TGF-β1-treated and untreated LLC cells. *HDAC2* gene expression was found to be significantly higher than the other *HDACs* (Fig. 2A). To validate whether *HDAC2* is the target gene, we compared mRNA and protein expression levels of HDACs between control (untreated) mice and those treated with BLM (3.5 mg/kg) for 28 days. We observed a significant reduction in *HDAC4, HDAC5, HDAC7,* and *HDAC9* mRNA and protein levels in BLM-treated mice compared to the control group. In contrast, *HDAC1*, *HDAC2*, *HDAC3*, *HDAC6*, *HDAC8*, and *HDAC10* mRNA

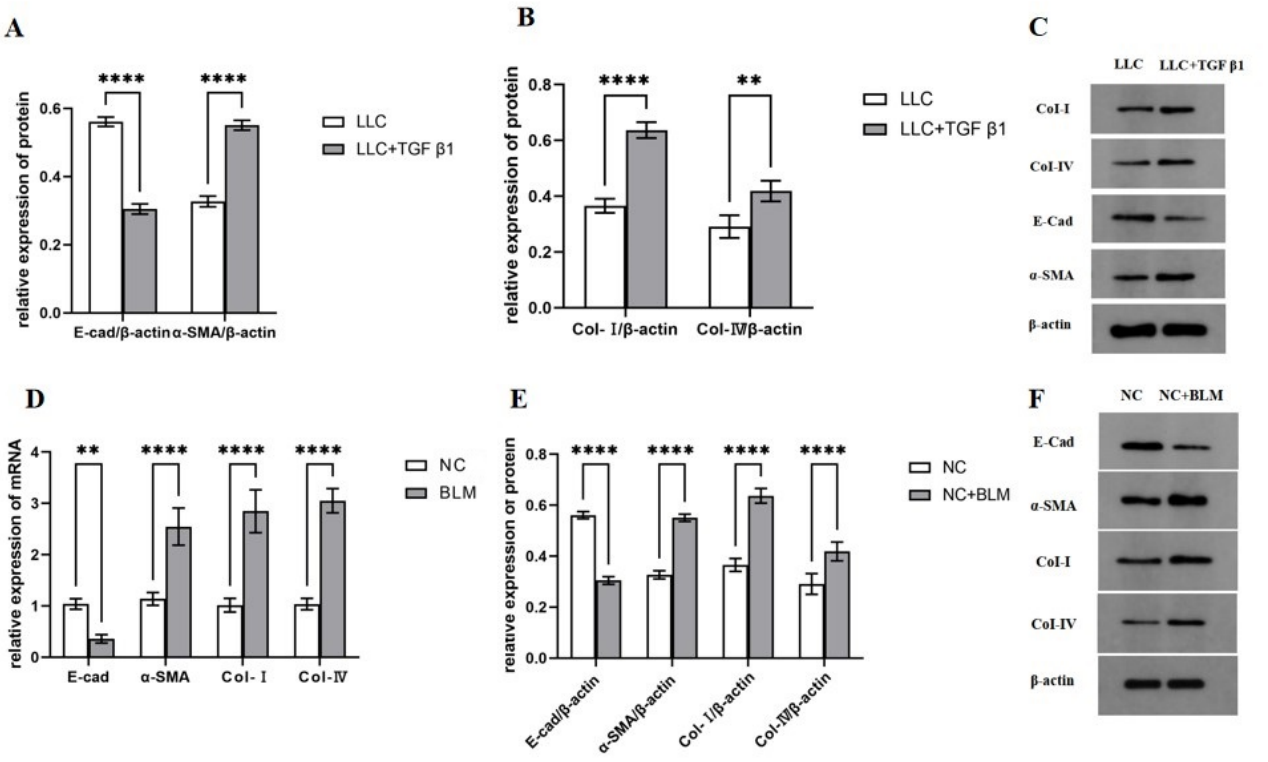

Fig. 1. The cell model of pulmonary fibrosis was established by treating LLC cells with TGF-β1 (5 ng/mL). C57BL/6 mice were intratracheally instilled with bleomycin to induce pulmonary fibrosis. (A) Protein levels of the EMT indicators, E-cad, and α-SMA were observed using WB. Expression levels of target genes were normalized to β-actin. (B,C) Protein levels of type I and type II collagens, which are indicators of fibrosis, were assessed using WB. (D–F) C57 mice were intratracheally instilled with bleomycin (3.5 mg/kg), and their lung tissues were collected after 28 days to evaluate the gene and protein expressions of EMT indicators and pulmonary fibrosis. Each experiment was independently replicated three times and the data were presented as means ± SD; n = 3/group; $**p < 0.01$, $****p < 0.0001$. EMT, epithelial-mesenchymal transition; LLC, lewis lung carcinoma; TGF-β1, transforming growth factor-β1; Col-I, collagen type I; Col-IV, collagen type IV; NC, Normal group; E-cad, E-cadherin; α-SMA, α-smooth muscle actin; WB, Western blotting; SD, standard deviation.

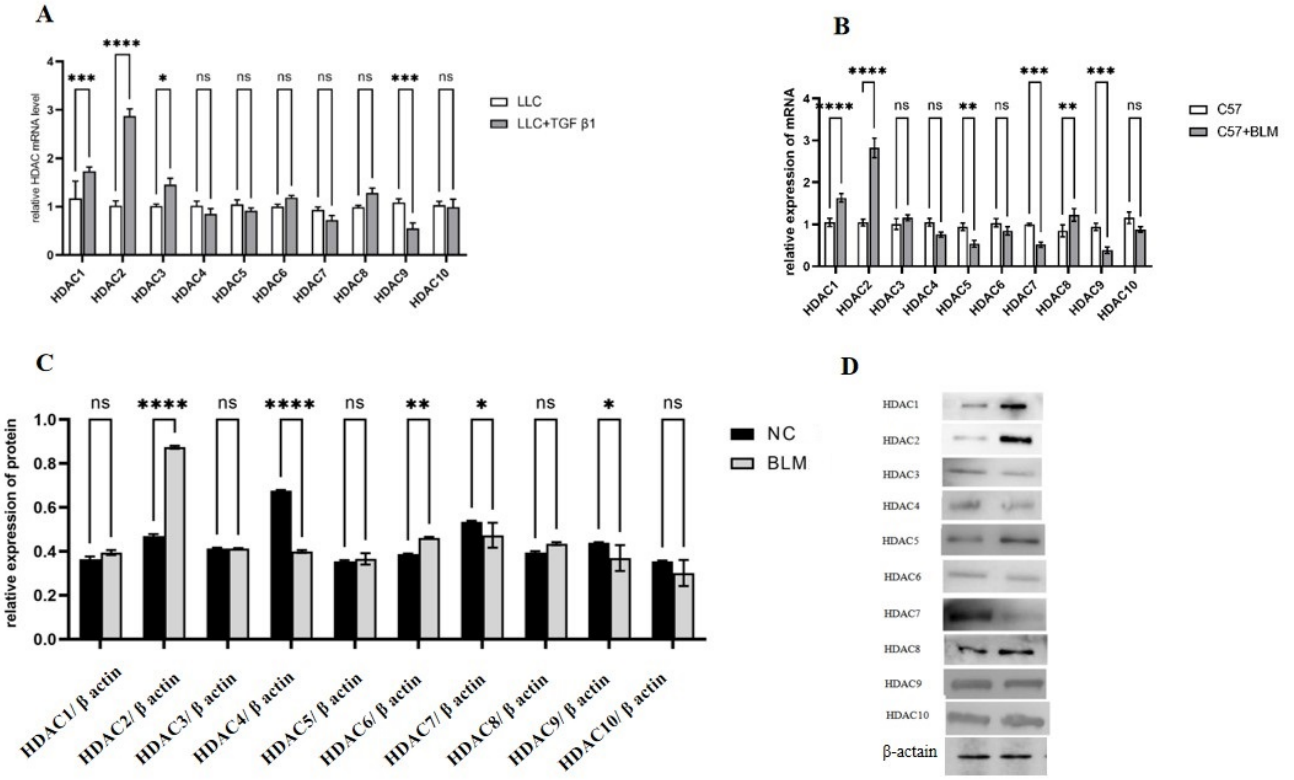

Fig. 2. Changes in histone deacetylases (HDACs) 1–10 during the epithelial-mesenchymal transition in pulmonary fibrosis. (A) Changes in *HDAC1–10* mRNA levels (assessed using qPCR) induced by TGF-β in LLC cells. (B–D) *HDAC 1–10* mRNA levels (assessed using qPCR) and protein levels in control and bleomycin (BLM)-treated mice detected by qPCR (B) and Western blot analysis (C,D). The data were presented as means ± SD, n = 3/group, *$p < 0.05$, **$p < 0.01$, ***$p < 0.001$, ****$p < 0.0001$, *ns* stands for no significant difference. qPCR, quantitative PCR.

and protein expression levels were increased. Importantly, the expression level of HDAC2 was comparatively higher than the other HDACs (Fig. 2B–D). Hence, HDAC2 was selected as the target for subsequent analysis.

Efficiency of Adenovirus Interference with HDAC2 after Infection of LLC Cells

The impact of HDAC2 on pulmonary fibrosis was assessed by three specific interference fragments: Hdac2-mus-231, Hdac2-mus-1021, and Hdac2-mus-1428. Each interference fragment was individually transfected into LLC cells. After 48 hours, green fluorescent protein expression was detected in LLC cells, accompanied by cellular rounding and partial fusion, indicating successful infection (Fig. 3A). The efficiency of adenovirus interference on HDAC2 expression in LLC cells was analyzed using qPCR. HDAC expression levels in Hdac2-mus-231-infected LLC cells were significantly lower than those in Hdac2-mus-1021 or Hdac2-mus-1428 infected cells or non-transfected control LLC cells (Fig. 3B). These results indicate the successful suppression of HDAC2 expression in LLC cells by Hdac2-mus-231 interference fragment.

Effects of Changes in HDAC2 on EMT and PF

After stimulation of LLC cells with TGF-β1, a significant reduction in HDAC2 expression was observed due to gene disruption. Subsequently, we evaluated the mRNA and protein levels of EMT and fibrosis markers. Knockdown of HDAC2 expression attenuated the changes in EMT and fibrosis markers induced by TGF-β1 in LLC cells. Particularly, the increased expression levels of α-SMA, Col-I, and Col-IV stimulated by TGF-β1 were significantly reduced in cells infected with Hdac2-mus-231, while the decreased expression of E-cadherin induced by TGF-β1 was significantly increased in cells infected with Hdac2-mus-231 (Fig. 4A–C).

The results of H&E staining from BLM-treated C57 mice are shown in Fig. 4G. Lung tissues of mice treated with BLM showed elevated presence of myofibroblasts and collagen fibroblasts compared to the control group. Moreover, disruption of alveolar structure, fusion of alveoli, widening and thickening of alveolar septa, and significant peri-airway changes were detected in the BLM-treated mice but not in the control group. Reducing the expression of HDAC2 effectively attenuated the signs of pulmonary fibrosis. Masson trichrome staining (Fig. 4G) showed fibrotic tissue in

Journal of
BIOLOGICAL REGULATORS
and Homeostatic Agents

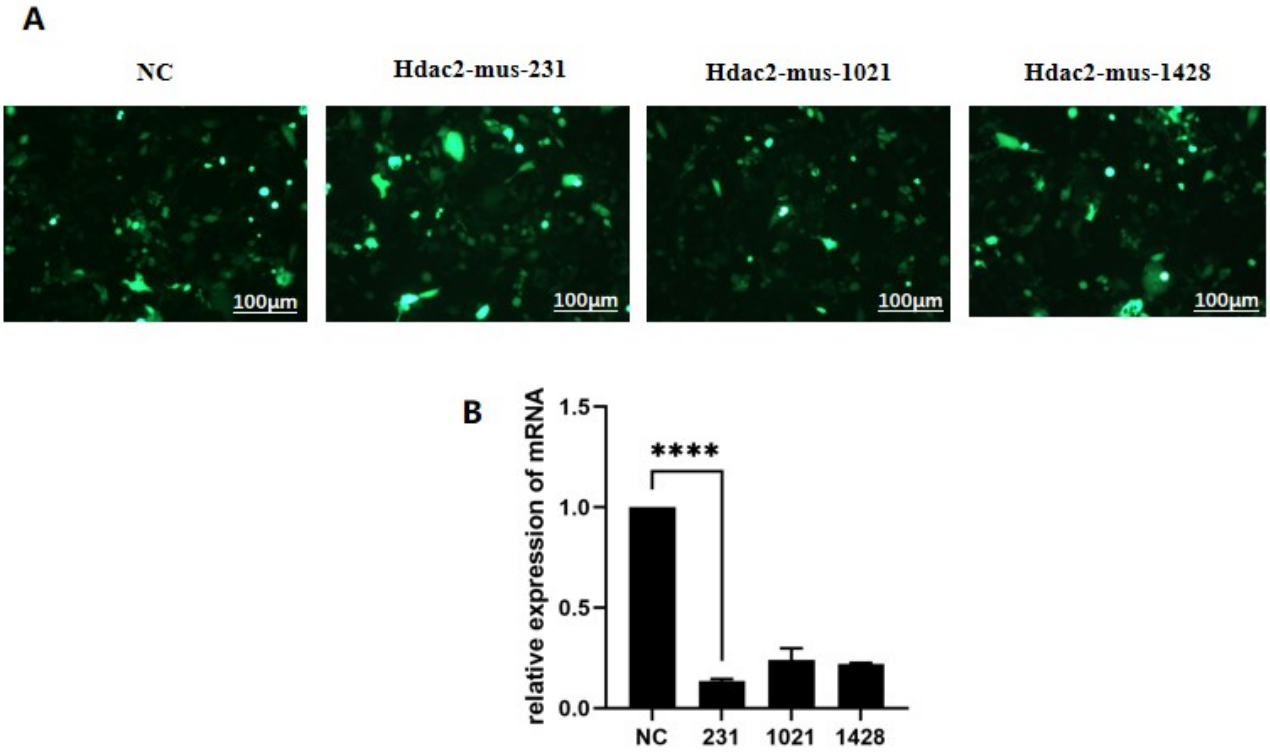

Fig. 3. The construction of an interfering virus targeting HDAC2 and infection of LLC cells for target screening. (A) LLC cells were infected with Hdac2-mus-231, Hdac2-mus-1021, and Hdac2-mus-1428 interfering fragments. After 48 hours, the expression levels of green fluorescent protein were observed through fluorescence microscopy, indicating pathological effects. (B) Infection with Hdac2-mus-231, Hdac2-mus-1021, and Hdac2-mus-1428 interfering fragments significantly decreased *HDAC2* gene expression in LLC cells. Comparatively, Hdac2-mus-231 infection resulted in a more pronounced decrease in *HDAC* gene expression. ****$p < 0.0001$.

the lungs of BLM-treated mice, characterized by the formation of continuous fibrotic septa and deposition of blue collagen fiber. Moreover, after knocking down HDAC2 expression, a significant reduction in the area of fibrotic fibers was found.

These findings indicate that reducing HDAC2 significantly inhibits EMT and reduces the degree of pulmonary fibrosis. Therefore, we inferred that HDAC2 plays a negative regulatory role in EMT and pulmonary fibrosis. Furthermore, the expression levels of α-SMA, E-Cad, Col-I, and Col-IV in lung tissues after HDAC2 knockdown were analyzed using qPCR and WB. The findings from *in vivo* experiment were consistent with those from *in vitro* analysis (Fig. 4D–F). These findings indicate that HDAC2 promotes EMT, and inhibiting the expression of HDAC2 can impede EMT and suppress the development of pulmonary fibrosis.

The changes in hydroxyproline levels in cells and lung tissue are shown in Fig. 4H,I. After stimulation with TGF-β1, the content of hydroxyproline in cells and mice significantly increased compared to the Virus group. Knocking down the expression of HDC2 can reduce the content of hydroxyproline in LLC cells and mouse lung tissue, and alleviate the degree of pulmonary fibrosis.

Knockdown of HDAC2 Reduced EGFR Synthesis and Inhibited p38/JNK MAPK Signaling

We explored the regulatory role of HDACs in the p38/JNK signaling pathway during pulmonary fibrosis development. Our findings showed that diminishing HDAC2 expression led to a decrease in the upregulation of epidermal growth factor receptor (EGFR), JNK, and p38, which was initially induced by TGF-β1 in LLC cells (refer to Fig. 5A,B). Additionally, HDAC2 knockdown resulted in a reduction of the elevated levels of phosphorylated JNK and p38, also induced by TGF-β1 in LLC cells (refer to Fig. 5C,D).

Discussion

The study investigated the role of class I and II HDACs in organ fibrosis [28]. For example, the overexpression of HDAC3 has been shown to promote renal fibrosis [29], and the upregulation of HDAC6 is linked to cardiac fibrosis [30]. However, the changes and underlying molecular mechanisms of HDACs 1–10 in the pathogenesis of pulmonary fibrosis remain unclear. We identified HDAC2 as the predominant HDAC involved in the development of pulmonary fibrosis. This study aimed to investigate the role

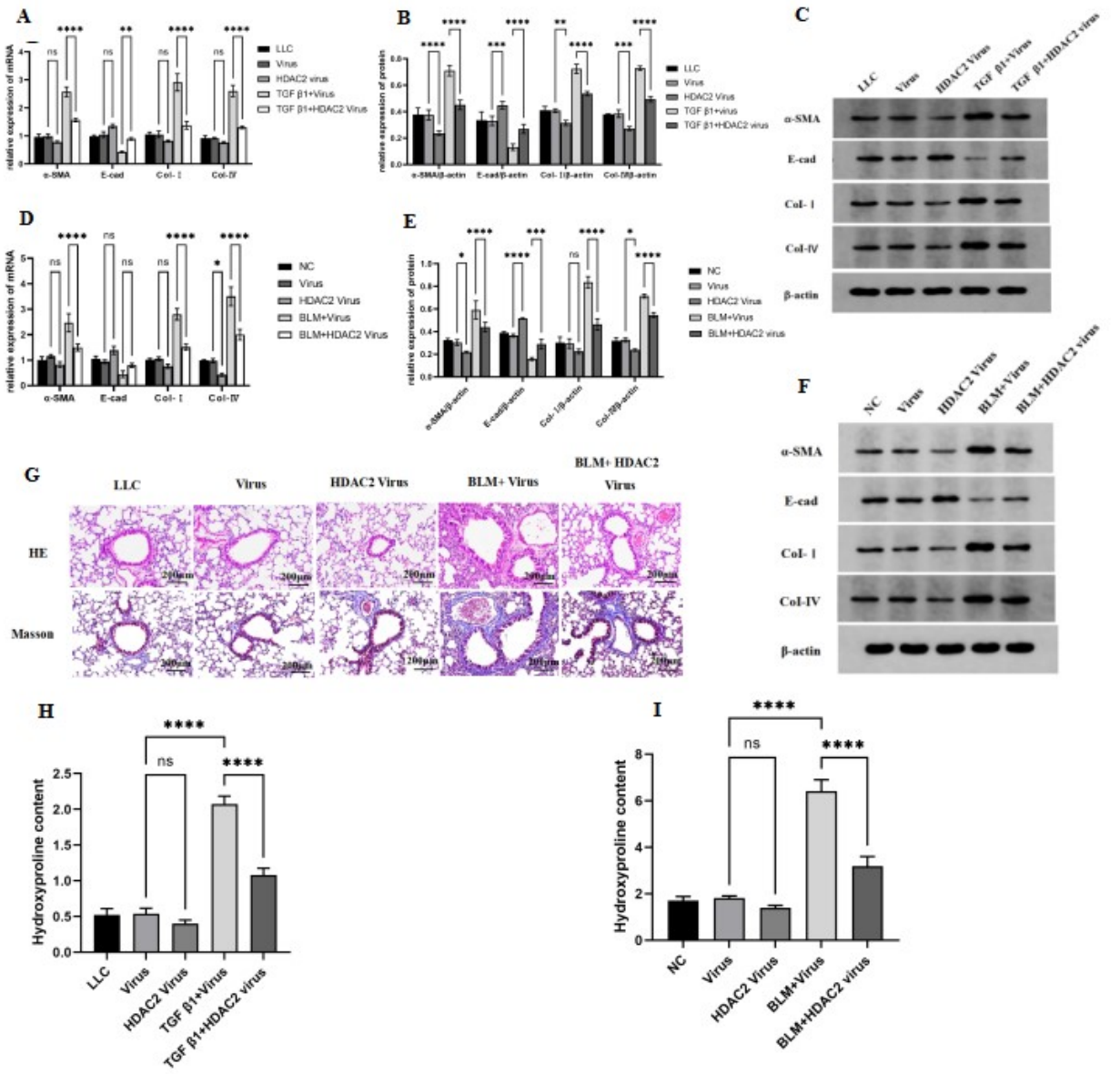

Fig. 4. Decreased HDAC2 expression suppresses pulmonary fibrosis induced by TGF-β1 or BLM. (A–C) In a cell model of pulmonary fibrosis induced by TGF-β1, knocking down HDAC2 expression suppresses EMT and inhibits the development of fibrosis. (D–F) Reduced HDAC expression attenuated the changes in EMT and fibrosis-associated markers induced by BLM. (G) Lung tissue sections were stained using hematoxylin and eosin (H&E) and Masson's trichrome stain, and images were captured using a light microscope. The original magnification was ×200. Hematoxylin and eosin staining showed significant muscle and collagen fibroblasts in the lung tissue of BLM-treated mice but not in the control groups. Knocking down HDAC2 expression attenuated the alveolar thickening and pulmonary fibrosis development induced by BLM. Masson staining showed significant pulmonary fibrosis induced by BLM, indicating continuous fibrosis intervals. Knocking down HDAC2 expression significantly reduced the fibrotic area. Changes in hydroxyproline levels in cells and lung tissue (H,I). The data were presented as means ± SD, n = 3/group, *$p < 0.05$, **$p < 0.01$, ***$p < 0.001$, ****$p < 0.0001$, *ns* indicates no significant difference.

of HDAC2 in the development of lung fibrosis and determine the underlying mechanisms.

Among HDACs 1–10, HDAC2 exhibited the most pronounced change in expression following TGF-β1 stimulation in LLC cells. The role of HDAC2 in the development of fibrosis was confirmed by a mouse model of BLM-induced lung fibrosis. Furthermore, reducing HDAC2 expression inhibited the development of pulmonary fibrosis. Reducing HDAC2 expression attenuated EMT and fibrosis markers induced by TGF-β1 and BLM in cell and mouse models of pulmonary fibrosis, respectively. SMA was reduced, the expression of E-cad was increased, and the ex-

Journal of
BIOLOGICAL REGULATORS
and Homeostatic Agents

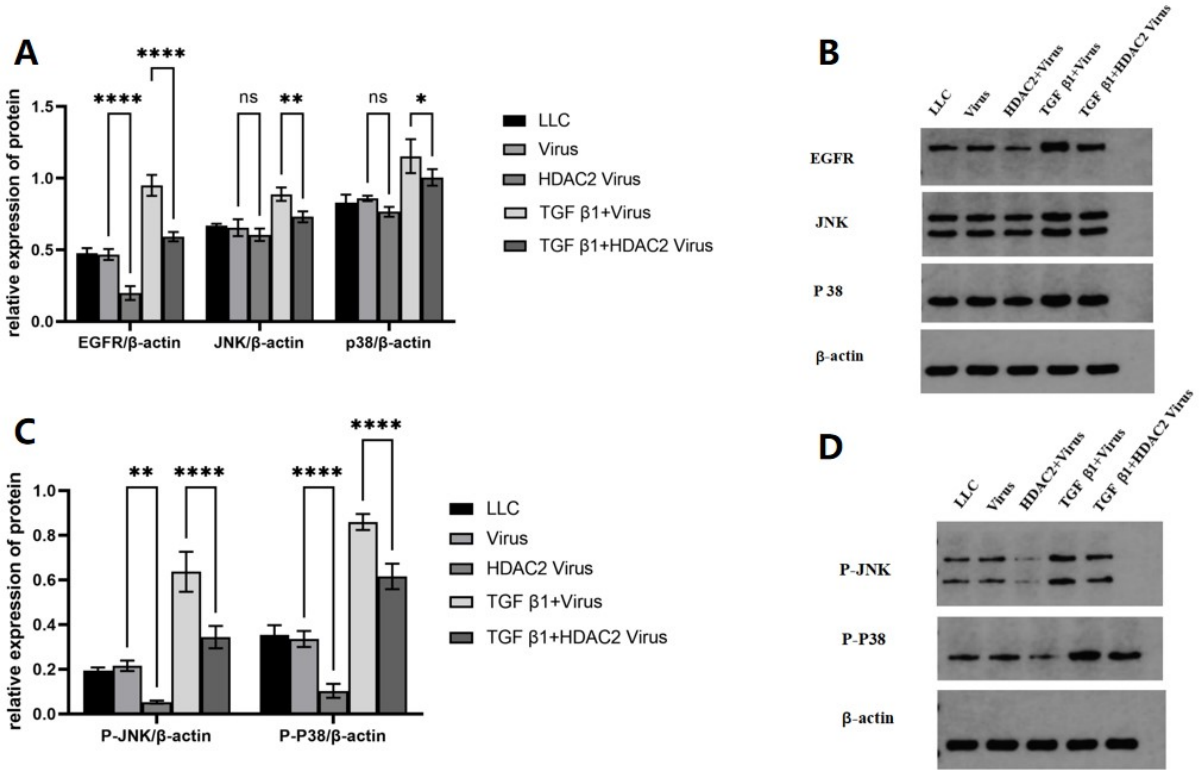

Fig. 5. Knocking down the expression of HDAC2 suppressed EGFR synthesis induced by TGF-β1 *in vitro*, thereby inhibiting the JNK/p38 MAPK signaling pathway. (A,B) Changes in EGFR, JNK, and p38 proteins in response to knockdown of HDAC2 after TGF-β1 stimulation in LLC cells. (C,D) Changes in phosphorylated JNK and p38 levels in response to knockdown of HDAC2 after TGF-β1 stimulation in LLC cells. The data were presented as means ± SD, n = 3/group, *$p < 0.05$, **$p < 0.01$, ****$p < 0.0001$, *ns* indicates no significant difference. EGFR, epidermal growth factor receptor; MAPK, mitogen-activated protein kinases; JNK, c-Jun N-terminal kinase.

pressions of Col-I and Col-IV were reduced by HDAC knockdown. These findings indicate that HDAC knockdown reduces the synthesis of fibrotic collagen, thereby inhibiting lung fibrosis.

Mechanistically, there is a positive correlation between EGFR expression and the degree of lung fibrosis [31]. Xiaochen Li *et al*. [32] demonstrated that TGF-β1 induces EGFR expression, stimulating fibroblast or myofibroblast transformation through the MAPK/extracellular regulated protein kinases (ERK) signaling pathway [29]. Recent studies have shown that HDAC2 knockdown inhibits EGFR synthesis and prevents downstream signaling by downregulating JNK and p38 expression. Therefore, our results indicate that TGF-β1 stimulates EGFR synthesis in LLC cells, and HDAC2 knockdown inhibits EGFR synthesis, thereby mitigating pulmonary fibrosis mediated by the JNK/p38 MAPK signaling pathway. These novel findings provide the basis for potential new treatments targeting pulmonary fibrosis interstitial lung disease.

This study has several limitations that must be addressed in subsequent investigations. Although reducing HDC2 expression attenuates epithelial-mesenchymal transition in pulmonary fibrosis and inhibits the JNK/p38 MAPK signaling pathway, additional aspects need comprehensive elucidation. For example, it remains unclear whether the expression of HDAC2 affects the expression of other HDACs, which may potentially impact pulmonary fibrosis. Furthermore, this study only observed the effect of reducing HDAC2 expression on pulmonary fibrosis, while it is unclear whether exogenous supplementation of HDAC2 affects the progression of pulmonary fibrosis, and the impact of abnormally elevated HDAC2 on pulmonary fibrosis remains unclear. Our research group plans to address all these questions in our future investigation to further enhance our understanding.

Conclusions

We observed significant changes in HDAC expression during the development of PF and identified the most pronounced changes in HDAC2. Furthermore, our findings demonstrate that HDAC2 knockdown can effectively inhibit EMT and attenuate PF. These findings highlight the significance of HDAC2 as a novel therapeutic target for interstitial lung disease associated with PF.

Availability of Data and Materials

All experimental data included in this study can be obtained by contacting the corresponding author if needed.

Author Contributions

YL was responsible for experimental design. WB assay, and manuscript writing. SS was responsible for qPCR assay and data collection. YT was responsible for collecting and analyzing data. SW made the figures and assisted experimentation. PZ provided important feedback and assisted experimentation. JH and YZ do data analysis. SR was responsible for conceptualization and experimental design, obtaining funding, writing the manuscript, and final review. YL draft the manuscript. All authors contributed to important editorial changes in the manuscript. All authors read and approved the final manuscript. All authors have participated sufficiently in the work and agreed to be accountable for all aspects of the work.

Ethics Approval and Consent to Participate

The study design was approved by the Animal Ethics Committee of Guizhou Medical University, China (No. 2101491) on 8 August 2021.

Acknowledgment

Not applicable.

Funding

This research was supported by the Science and Technology Funding of Guizhou province (Grant No. [2021]054; [2016]2907).

Conflict of Interest

The authors declare no conflict of interest.

References

[1] Liu D, Zhu H, Gong L, Pu S, Wu Y, Zhang W, *et al*. Histone Deacetylases Promote ER Stress Induced Epithelial Mesenchymal Transition in Human Lung Epithelial Cells. Cellular Physiology and Biochemistry: International Journal of Experimental Cellular Physiology, Biochemistry, and Pharmacology. 2018; 46: 1821–1834.

[2] Diedrich D, Stenzel K, Hesping E, Antonova-Koch Y, Gebru T, Duffy S, *et al*. One-pot, multi-component synthesis and structure-activity relationships of peptoid-based histone deacetylase (HDAC) inhibitors targeting malaria parasites. European Journal of Medicinal Chemistry. 2018; 158: 801–813.

[3] Chen F, Gao Q, Wei A, Chen X, Shi Y, Wang H, *et al*. Histone deacetylase 3 aberration inhibits Klotho transcription and promotes renal fibrosis. Cell Death and Differentiation. 2021; 28: 1001–1012.

[4] Gediya P, Parikh PK, Vyas VK, Ghate MD. Histone deacetylase 2: A potential therapeutic target for cancer and neurodegenerative disorders. European Journal of Medicinal Chemistry. 2021; 216: 113332.

[5] Zhang W, Zhang Q, Zhu Y, Zhang Y, Xia Y, Wei Z, *et al*. Rectal administration of butyrate ameliorates pulmonary fibrosis in mice through induction of hepatocyte growth factor in the colon via the HDAC-PPARγ pathway. Life Sciences. 2022; 309: 120972.

[6] Saito S, Zhuang Y, Suzuki T, Ota Y, Bateman ME, Alkhatib AL, *et al*. HDAC8 inhibition ameliorates pulmonary fibrosis. American Journal of Physiology. Lung Cellular and Molecular Physiology. 2019; 316: L175–L186.

[7] Zhang Z, Qu J, Zheng C, Zhang P, Zhou W, Cui W, *et al*. Nrf2 antioxidant pathway suppresses Numb-mediated epithelial-mesenchymal transition during pulmonary fibrosis. Cell Death & Disease. 2018; 9: 83.

[8] Ji Y, Dou YN, Zhao QW, Zhang JZ, Yang Y, Wang T, *et al*. Paeoniflorin suppresses TGF-β mediated epithelial-mesenchymal transition in pulmonary fibrosis through a Smad-dependent pathway. Acta Pharmacologica Sinica. 2016; 37: 794–804.

[9] Noh H, Oh EY, Seo JY, Yu MR, Kim YO, Ha H, *et al*. Histone deacetylase-2 is a key regulator of diabetes- and transforming growth factor-beta1-induced renal injury. American Journal of Physiology. Renal Physiology. 2009; 297: F729–F739.

[10] Glenisson W, Castronovo V, Waltregny D. Histone deacetylase 4 is required for TGFbeta1-induced myofibroblastic differentiation. Biochimica et Biophysica Acta. 2007; 1773: 1572–1582.

[11] Goodwin CM, Waters AM, Klomp JE, Javaid S, Bryant KL, Stalnecker CA, *et al*. Combination Therapies with CDK4/6 Inhibitors to Treat KRAS-Mutant Pancreatic Cancer. Cancer Research. 2023; 83: 141–157.

[12] Lin YH, Major JL, Liebner T, Hourani Z, Travers JG, Wennersten SA, *et al*. HDAC6 modulates myofibril stiffness and diastolic function of the heart. The Journal of Clinical Investigation. 2022; 132: e148333.

[13] Liu W, Han X, Li Q, Sun L, Wang J. Iguratimod ameliorates bleomycin-induced pulmonary fibrosis by inhibiting the EMT process and NLRP3 inflammasome activation. Biomedicine & Pharmacotherapy. 2022; 153: 113460.

[14] Minagawa S, Araya J, Numata T, Nojiri S, Hara H, Yumino Y, *et al*. Accelerated epithelial cell senescence in IPF and the inhibitory role of SIRT6 in TGF-β-induced senescence of human bronchial epithelial cells. American Journal of Physiology. Lung Cellular and Molecular Physiology. 2011; 300: L391–L401.

[15] Hu L, Yu Y, Huang H, Fan H, Hu L, Yin C, *et al*. Epigenetic Regulation of Interleukin 6 by Histone Acetylation in Macrophages and Its Role in Paraquat-Induced Pulmonary Fibrosis. Frontiers in Immunology. 2017; 7: 696.

[16] Hsu DSS, Wang HJ, Tai SK, Chou CH, Hsieh CH, Chiu PH, *et al*. Acetylation of snail modulates the cytokinome of cancer cells to enhance the recruitment of macrophages. Cancer Cell. 2014; 26: 534–548.

[17] Li M, Zheng Y, Yuan H, Liu Y, Wen X. Effects of dynamic changes in histone acetylation and deacetylase activity on pulmonary fibrosis. International Immunopharmacology. 2017; 52: 272–280.

[18] Chen L, Alam A, Pac-Soo A, Chen Q, Shang Y, Zhao H, *et al*. Pretreatment with valproic acid alleviates pulmonary fibrosis through epithelial-mesenchymal transition inhibition *in vitro* and *in vivo*. Laboratory Investigation; a Journal of Technical Methods and Pathology. 2021; 101: 1166–1175.

[19] Lyu X, Hu M, Peng J, Zhang X, Sanders YY. HDAC inhibitors as antifibrotic drugs in cardiac and pulmonary fibrosis. Therapeutic Advances in Chronic Disease. 2019; 10: 2040622319862697.

[20] Zhang L, Han Y, Jiang Q, Wang C, Chen X, Li X, *et al*. Trend of histone deacetylase inhibitors in cancer therapy: isoform se-

lectivity or multitargeted strategy. Medicinal Research Reviews. 2015; 35: 63–84.

[21] Wattanathamsan O, Chantaravisoot N, Wongkongkathep P, Kungsukool S, Chetprayoon P, Chanvorachote P, *et al*. Inhibition of histone deacetylase 6 destabilizes ERK phosphorylation and suppresses cancer proliferation via modulation of the tubulin acetylation-GRP78 interaction. Journal of Biomedical Science. 2023; 30: 4.

[22] Seto E, Yoshida M. Erasers of histone acetylation: the histone deacetylase enzymes. Cold Spring Harbor Perspectives in Biology. 2014; 6: a018713.

[23] Wang H, Fu BB, Gale RP, Liang Y. NK-/T-cell lymphomas. Leukemia. 2021; 35: 2460–2468.

[24] Snyder RO, Flotte TR. Production of clinical-grade recombinant adeno-associated virus vectors. Current Opinion in Biotechnology. 2002; 13: 418–423.

[25] Knop DR, Harrell H. Bioreactor production of recombinant herpes simplex virus vectors. Biotechnology Progress. 2007; 23: 715–721.

[26] Rao SS, Zhang XY, Shi MJ, Xiao Y, Zhang YY, Wang YY, *et al*. Suberoylanilide hydroxamic acid attenuates paraquat-induced pulmonary fibrosis by preventing Smad7 from deacetylation in rats. Journal of Thoracic Disease. 2016; 8: 2485–2494.

[27] Bin YF, Wu LJ, Sun XJ, Liang Y, Bai J, Zhang JQ, *et al*. Expression of GR-α and HDAC2 in steroid-Sensitive and steroid-Insensitive interstitial lung disease. Biomedicine & Pharmacotherapy. 2019; 118: 109380.

[28] Jeong SH, Son ES, Lee YE, Kyung SY, Park JW, Kim SH. Histone deacetylase 3 promotes alveolar epithelial-mesenchymal transition and fibroblast migration under hypoxic conditions. Experimental & Molecular Medicine. 2022; 54: 922–931.

[29] Wang J, He F, Chen L, Li Q, Jin S, Zheng H, *et al*. Resveratrol inhibits pulmonary fibrosis by regulating miR-21 through MAPK/AP-1 pathways. Biomedicine & Pharmacotherapy = Biomedecine & Pharmacotherapie. 2018; 105: 37–44.

[30] Cheng WH, Kao SY, Chen CL, Yuliani FS, Lin LY, Lin CH, *et al*. Amphiregulin induces CCN2 and fibronectin expression by TGF-β through EGFR-dependent pathway in lung epithelial cells. Respiratory Research. 2022; 23: 381.

[31] Jänne PA, Yang JC, Kim DW, Planchard D, Ohe Y, Ramalingam SS, *et al*. AZD9291 in EGFR inhibitor-resistant non-small-cell lung cancer. The New England Journal of Medicine. 2015; 372: 1689–1699.

[32] Li X, Cao X, Zhao H, Guo M, Fang X, Li K,*et al*. Hypoxia Activates Notch4 via ERK/JNK/P38 MAPK Signaling Pathways to Promote Lung Adenocarcinoma Progression and Metastasis. Frontiers in Cell and Developmental Biology. 2021; 9: 780121.